Journal of Vertebrate Paleontology

ISSN: 0272-4634 (Print) 1937-2809 (Online) Journal homepage: www.tandfonline.com/journals/ujvp20

Classification of dinosaur footprints using machine learning

Michael Jones, Jens N. Lallensack, Ian Jarman, Peter Falkingham & Ivo Siekmann

To cite this article: Michael Jones, Jens N. Lallensack, Ian Jarman, Peter Falkingham & Ivo Siekmann (09 May 2025): Classification of dinosaur footprints using machine learning, Journal of Vertebrate Paleontology, DOI: 10.1080/02724634.2025.2493157

To link to this article: https://doi.org/10.1080/02724634.2025.2493157

© 2025 Michael Jones, Jens N. Lallensack, Ian Jarman, Peter Falkingham, Ivo Siekmann. Published with license by the Society of Vertebrate Paleontology

View supplementary material

Published online: 09 May 2025.

Submit your article to this journal

Article views: 269

View related articles

View Crossmark data

Full Terms & Conditions of access and use can be found at https://www.tandfonline.com/action/journalInformation?journalCode=ujvp20

Journal of Vertebrate Paleontology e2493157 (12 pages)
Published with license by the Society of Vertebrate Paleontology
DOI: 10.1080/02724634.2025.2493157

Check for updates

ARTICLE

CLASSIFICATION OF DINOSAUR FOOTPRINTS USING MACHINE LEARNING

MICHAEL JONES,[1] JENS N. LALLENSACK, [2] IAN JARMAN, [1] PETER FALKINGHAM, [3] and IVO SIEKMANN [1]*
[1]School of Computer Science and Mathematics (CSM), Faculty of Engineering and Technology (FET), Liverpool John Moores University (LJMU), Liverpool L3 3AF, U.K., i.siekmann@ljmu.ac.uk;
[2]Departamento de Ciência da Computação, Universidade Federal de Minas Gerais, Av. Antônio Carlos, 6627 31270-901, Belo Horizonte, Minas Gerais, Brasil;
[3]School of Biological and Environmental Sciences (BES), Faculty of Science, Liverpool John Moores University (LJMU), Liverpool L3 3AF, U.K.

ABSTRACT—Fossilized dinosaur footprints enable us to study the behavior of individual dinosaurs as well as interactions between dinosaurs of the same or different species. There are two principal groups of three-toed dinosaurs, ornithopods and theropods. Determining if a footprint is from an ornithopod or a theropod is a challenging problem. Based on a data set of over 300 dinosaur footprints we train several machine learning models for classifying footprints as either ornithopods or theropods. The data are provided in the form of 20 landmarks for representing each footprint which are derived from images. Variable selection using logistic forward regression demonstrates that the selected landmarks are at locations that are intuitively expected to be especially informative locations, such as the top or the bottom of a footprint. Most models show good accuracy but the recall of ornithopods, of which fewer samples were contained in the data set, was generally lower than the recall of theropods. The Multi-Layer Perceptron (MLP) stands out as the model which did best at dealing with the class imbalance. Finally, we investigate which footprints were misclassified by the majority of models. We find that some misclassified samples exhibit features that are characteristic of the other class or have a compromised shape, for example, a middle toe that points to the left or the right rather than straight ahead.

SUPPLEMENTARY FILES—Supplementary files are available for this article for free at www.tandfonline.com/UJVP.

Citation for this article: Jones, M., Lallensack, J. N., Jarman, I., Falkingham, P., & Siekmann, I. (2025) Classification of dinosaur footprints using machine learning. *Journal of Vertebrate Paleontology*. https://doi.org/10.1080/02724634.2025.2493157

Submitted: June 28, 2024
Revisions received: March 31, 2025
Accepted: April 4, 2025

INTRODUCTION

Ornithopods and theropods are two groups of tridactyl (three-toed) dinosaurs. Whereas the herbivorous ornithopods went extinct at the end of the Cretaceous period, the primarily carnivorous theropods evolved into modern birds. Fossilized footprints are a valuable data source that can provide insight into the speed at which a dinosaur moved as well as more general traits of their behavior. Throughout the literature they have predominantly been reported as photographic images and outline tracings, though this has changed in recent years via the acquisition of 3D data (Falkingham et al., 2018). However, even when full 3D data are collected, these images are then often further simplified for statistical analysis by extracting morphological features such as lengths, widths, and angles. Throughout this article, when referring to tetrapod track data, we use the terminology recently proposed by Lallensack et al. (2025).

Broadly, the shapes of ornithopod and theropod footprints differ in various characteristics. Ornithopod footprints are usually wider and more symmetric than theropod footprints. Also, their middle toes (digit III) are commonly shorter i.e., they do not extend as far beyond the other toes (digits II and IV) as in theropods. However, these observations are unsuitable for defining general rules for distinguishing ornithopods and theropods because the characteristics described above can be found in both groups. Moreover, as Falkingham (2014) shows, the shape of a footprint is not only determined by the anatomy of the foot but also by the properties of the substrate as well as the dynamics of the dinosaur as it left the footprint; they refer to the influence of these three dimensions as the morphospace. Thus, determining if a given footprint is from an ornithopod or a theropod remains a difficult problem.

A prime example of this difficulty lies with the large tridactyl prints of Lark Quarry, Australia (Thulborn & Wade, 1979). Originally described as theropod in origin (Thulborn & Wade, 1979, 1984), the tracks were later reinterpreted by Romilio and Salisbury (2011) and Romilio et al. (2013) as having been made by an ornithopod. Key to this reinterpretation was Romilio et al.'s (2014) use of multivariate analysis techniques pioneered by Moratalla et al. (1988). This was later critiqued by Thulborn (2013), whose critique was again then questioned by Romilio and Salisbury (2014). Falkingham et al. (2016) subsequently demonstrated

*Corresponding author.
© 2025 Michael Jones, Jens N. Lallensack, Ian Jarman, Peter Falkingham, Ivo Siekmann. This is an Open Access article distributed under the terms of the Creative Commons Attribution License (http://creativecommons.org/licenses/by/4.0/), which permits unrestricted use, distribution, and reproduction in any medium, provided the original work is properly cited. The terms on which this article has been published allow the posting of the Accepted Manuscript in a repository by the author(s) or with their consent.

Color versions of one or more of the figures in the article can be found online at www.tandfonline.com/ujvp.

Published online 09 May 2025

that even applying the ostensibly 'objective' multivariate analysis resulted in highly subjective interpretations depending on where in the 3D geometry an 'outline' was picked, stressing that using a single outline in this way was flawed. Falkingham ultimately determined that the tracks were more theropod-like than ornithopod-like when considering the internal (deeper) outlines. These same tracks were revisited in Lallensack et al.'s (2022) first application of machine learning, where interpreted track-maker varied depending on which track, and whose outline was passed to the algorithm.

The aim of our study is to address this challenge by designing classifiers based on several machine learning methods. This has the additional benefit that the decision if a footprint is classified as an ornithopod or a theropod is based on statistical analysis of the data rather than on subjective decisions.

Several representative publications classify footprints by identifying clusters in scatter plots of various metrics (Castanera et al., 2013; Demathieu, 1990; dePolo et al., 2020; Figueiredo et al., 2017; Mateus & Milàn, 2008; Piñuela et al., 2016; Romilio & Salisbury, 2011; Schulp & Al-Wosabi, 2012; Thulborn, 2013), which relies on subjective decisions such as the selection of metrics to be considered as well as the definition of the cluster boundaries. The quantitative analysis of differences between ornithopods and theropods begins with the seminal study by Moratalla et al. (1988). The authors selected a sample of 66 tridactyl footprints from the Early Cretaceous period and originating from various geographic locations. They applied factor analysis (FA) and linear discriminant analysis (LDA) to features such as length and width of each digit with the aim to discriminate between theropods and ornithopods.

Lallensack et al. (2016) looked at three trackways from the Lower Cretaceous found in Münchehagen, Germany. The authors applied geometric morphometrics to footprint outlines and landmarks. They performed Principal Component Analysis (PCA) and found that asymmetry in the terminations of the digit impressions were a large distinguishing factor between the two groups. Lallensack (2019) extended this work by developing an algorithm that could automatically define the outline of a footprint. They tested this with a single theropod trackway from the same time period and geographic region as the trackways used by Lallensack et al. (2016). Lallensack et al. (2020) aimed to characterize the variability of footprint shapes over time and between theropods and ornithopods. The authors took 303 footprints originating from the Late Triassic period, through the Jurassic all the way to the Late Cretaceous period from 134 publications. The full data set used in this study is available in the Supplementary Material of this article. Each footprint was described by 34 landmarks and reference points and information such as the size was also recorded. They observed that ornithopod footprints are, on average, larger and wider than theropod footprints. Moreover, the features distinguishing theropods and ornithopods change with size, and the small ornithischian footprints are most similar in shape to large theropod footprints. Ornithischian footprints increased in size over time from the Early Jurassic to the Late Cretaceous period indicating an increase in body size over that time period, which, interestingly, is not observed in theropod footprints.

The data by Lallensack et al. (2020) will be used in this study for developing classification algorithms that enable us to automatically distinguish between ornithopod and theropod footprints. Rather than representing the expert knowledge of an ichnologist, our goal is to use machine learning for classification solely based on the geometric properties of the footprints. Thus, we will not be able to rely on additional criteria to distinguish theropods from ornithopods such as evidence for four-legged locomotion. In principle, our machine learning methods might therefore misclassify footprints that would be "obvious" for a paleontologist, but our approach has the advantage that we can determine how well theropod and ornithopods can be distinguished when using only the shapes of the footprints.

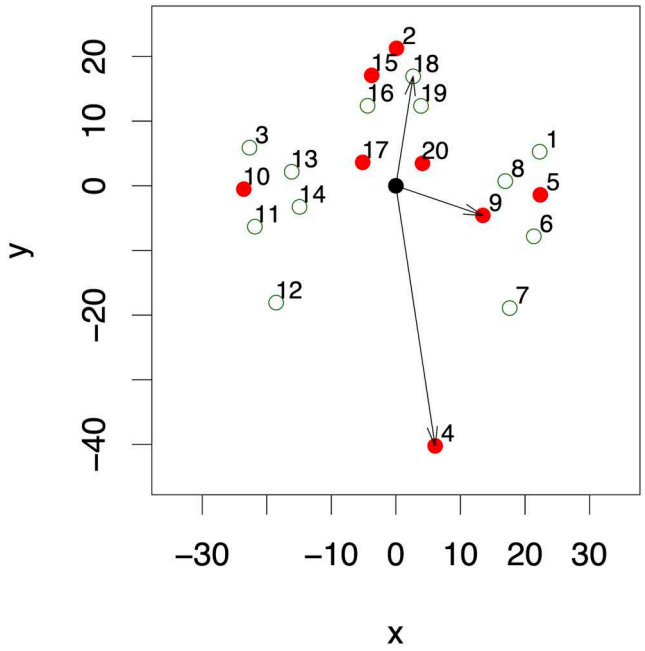

FIGURE 1. Example for a footprint from the data set by Lallensack et al. (2020) whose outline has been represented by 20 landmarks. The three arrows provide examples of how the coordinates (x, y) of landmarks (here shown for the examples 4, 9, and 18) are converted to distances r from the center. The landmarks shown as filled circles were selected by variable selection via forward step logistic regression.

Although we use a substantially smaller data set than Lallensack et al. (2022), the Multi-Layer Perceptron (MLP), our best-performing method, demonstrates good performance on the test set with recall of ornithopods and theropods of 90.0% and 89.5%, respectively, and an accuracy of 90%. Whilst the deep learning network proposed by Lallensack et al. (2022) is trained on black and white "silhouettes," each footprint in our data set is represented by just 20 landmarks that are placed in meaningful locations of a footprint such as the tips of any of the three toes. This pre-processing of the data enables us to use computationally much less expensive models such as logistic regression, random forest or multilayer perceptron which require much smaller training data sets than complex neural network architectures.

MATERIALS AND METHODS

The classification methods developed in this study are based on a data set that represents the visual features of dinosaur footprints by a system of landmarks (Lallensack et al., 2020). Lallensack et al. (2020) collected images of 303 dinosaur footprints from 134 different publications and represented the outline of each dinosaur footprint by 20 landmarks, see Figure 1. Two of the 303 footprints were not labeled as ornithopods or theropods, so these two samples were omitted. The remaining data set consists of 301 footprints, 108 labeled ornithopods, 193 labeled theropods. Because the footprints originate from a wide range of sources and were classified by many different paleontologists it is unlikely that the classifications are influenced by a strong bias. The full

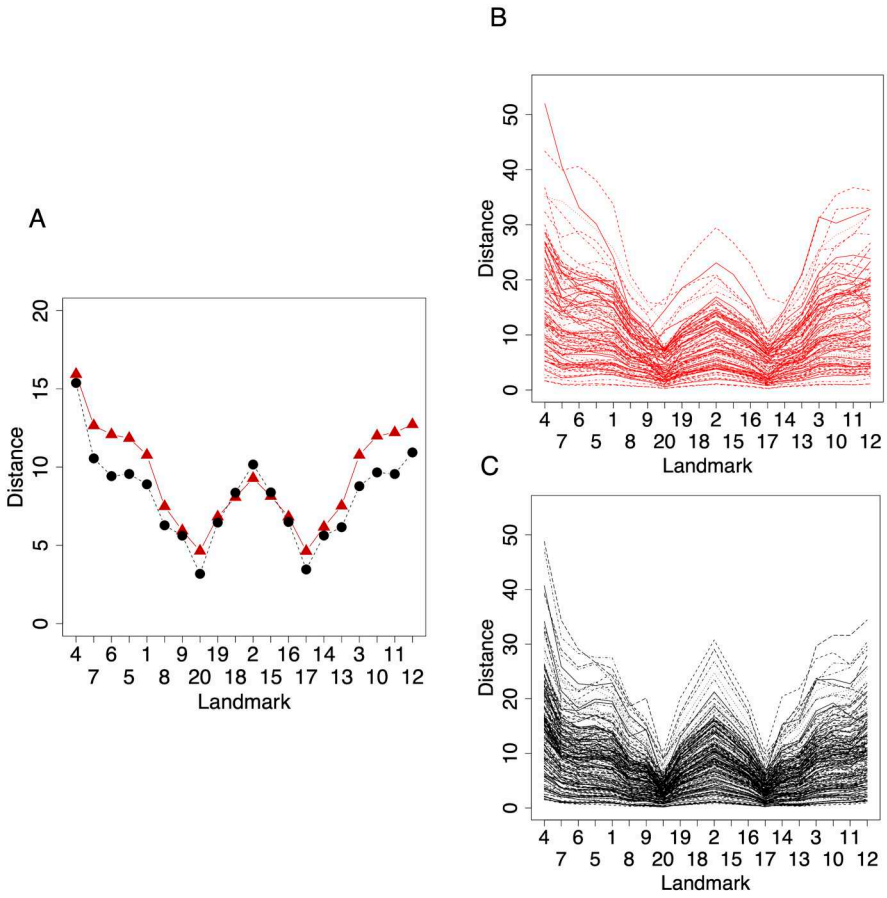

FIGURE 2. Visualization of the data set by Lallensack et al. (2020) after transforming the two-dimensional coordinates to distances r from the origin $(0, 0)$ according to equation (1). In the plots, also the sequence of the landmarks is changed, starting with landmark 4 on the left of the x axis and then moving counter-clockwise along the boundary of the footprint. In **A**, the means of the distances r is plotted for all 20 landmarks for ornithopods (triangles) and theropods (circles). The distances r for all ornithopods are shown in **B**, theropods are shown in **C**.

data set is available in the Supplementary Material. As can be seen in Figure 1, each of the 20 landmarks is represented as a point (x, y) in a two-dimensional coordinate system. We simplify the data set by transforming each landmark (x, y) to its distance r from the center $(0, 0)$ as illustrated by the arrows in Figure 1:

$$(x,\ y) \mapsto r = \sqrt{x^2 + y^2}. \tag{1}$$

Thus, the number of variables is reduced from $2 \times 20 = 40$ to 20 variables. This transformed data set, see Figure 2, was then used for training models for classifying footprints as theropods or ornithopods, respectively. Please note that for the purposes of this visualization the sequence of distances from the center plotted in Figure 2 was changed, starting with landmark 4 on the left of the x-axis and then moving counter-clockwise along the boundary starting with landmark 4 and ending with landmark 12 (Figs. 1, 2).

The algorithms included in our study were Logistic Regression (LR), Multi-Layer Perceptron (MLP), Random Forest (RF), Support Vector Machine (SVM), Multivariate Adaptive Regression Splines (MARS) and Linear Discriminant Analysis (LDA). More details on these well-known machine learning methods can be found in standard textbooks such as, for example, Hastie et al. (2009). The following software implementations available as packages contained in the programming language R (R Core Team, 2023) were used: stats (LR), MASS (LDA), nnet (MLP), randomForestSRC (RF), e1071 (SVM), mda (MARS). The R implementation is available in the Supplementary Material as an R Markdown (Rmd) source file and a PDF report generated from the Rmd.

RESULTS

All results reported in this article can be reproduced using the R Markdown (Rmd) file made available as Supplementary Material. The mean distances of each landmark for ornithopods and theropods shown in Figure 2A already give some insight into the differences between the two classes. When comparing the solid curve representing the ornithopods and the dashed curve showing the theropods, landmarks 1, 5, 6, 7 on the right of the footprint, see Figure 1, and landmarks 3, 10, 11, and 12 on the left of the footprint, see Figure 1, are, on average, further away from the center for ornithopod footprints than for theropod footprints. These observations illustrate that ornithopod footprints are usually wider than theropod footprints. Carrying out a multivariate test that extends the two-sample t-test to multiple variables as described in Härdle and Simar (2014) it can be shown that the mean distances of the landmarks are significantly different ($\alpha = 0.05$) for ornithopods and theropods.

A slightly more subtle feature of Figure 2A relates to landmarks 2, 17, and 20. Here, the distances of landmarks 17 and 20 are again shorter for theropods but landmark 2 is on average further away from the center than the same landmark in ornithopods. Combining these two observations illustrates another distinguishing feature of the two classes, namely that the middle toe of a theropod is usually longer than the middle toe of an ornithopod.

TABLE 1. Performance of six classification methods that were trained on a training set of 211 samples of the data by Lallensack et al. (2020) determined by testing on the remaining 90 samples. For each method the first table shows confusion matrices as well as recall (the percentage of correctly classified samples) of ornithopods and theropods for the standard threshold of 0.5. The second table shows confusion matrices and recall values for an adjusted classification threshold obtained from the ROC curves shown in Figure 3. Finally, AUROC and classification accuracies before and after adjusting the thresholds are reported in the third table for each method. Plots of recall and accuracy for all methods before and after adjusting the thresholds are shown in Figure 4.

Forward Stepwise Logistic Regression (LR)

	Ornithopods	Theropods		Ornithopods	Theropods	Accuracy	
Ornithopods	25	10	Ornithopods	28	12	- before	80.0%
Theropods	8	47	Theropods	5	45	- after	81.1%
Recall	75.8%	82.5%	Recall	84.8%	78.9%	AUROC	0.902

Multi-Layer Perceptron (MLP)

	Ornithopods	Theropods		Ornithopods	Theropods	Accuracy	
Ornithopods	30	7	Ornithopods	30	6	- before	88.9%
Theropods	3	50	Theropods	3	51	- after	90%
Recall	90.9%	87.7%	Recall	90.9%	89.5%	AUROC	0.934

Linear Discriminant Analysis (LDA)

	Ornithopods	Theropods		Ornithopods	Theropods	Accuracy	
Ornithopods	23	5	Ornithopods	22	1	- before	83.3%
Theropods	10	52	Theropods	11	56	- after	86.7%
Recall	69.7%	91.2%	Recall	66.7%	98.2%	AUROC	0.901

Support Vector Machine (SVM)

	Ornithopods	Theropods		Ornithopods	Theropods	Accuracy	
Ornithopods	26	7	Ornithopods	28	9	- before	84.4%
Theropods	7	50	Theropods	5	48	- after	84.4%
Recall	78.8%	87.7%	Recall	84.8%	84.2%	AUROC	0.925

Random Forest (RF)

	Ornithopods	Theropods		Ornithopods	Theropods	Accuracy	
Ornithopods	25	7	Ornithopods	29	10	- before	83.3%
Theropods	8	50	Theropods	4	47	- after	84.4%
Recall	75.8%	87.7%	Recall	87.9%	82.5%	AUROC	0.888

Multivariate Adaptive Regression Splines (MARS)

	Ornithopods	Theropods		Ornithopods	Theropods	Accuracy	
Ornithopods	26	10	Ornithopods	29	10	- before	83.3%
Theropods	7	47	Theropods	4	47	- after	84.4%
Recall	78.8%	82.5%	Recall	87.9%	82.5%	AUROC	0.888

Altogether, the three panels of Figure 2 illustrate the shape of a three-toed footprint. From landmark 4 which marks the bottom of the footprint, the distance decreases along the right part of the footprint and along the right toe until a minimum is reached at the gap between the right and the middle toe (landmark 20). The distance then increases along the middle toe until the tip is reached (landmark 2). Left of landmark 2 the distance again decreases until the gap between the middle toe and the right toe is reached (landmark 17). Finally, the distance increases again along the left toe and the left side of the footprint. As we can see for both ornithopods (Figure 2B) and theropods (Figure 2C) the graphs for all footprints in the data set follow this pattern although they vary over a wide range. This is related to the footprint size, the distances increase with the footprint size.

In order to train the classifiers used in the study using Logistic Regression (LR), Multi-Layer Perceptron (MLP), Random Forest (RF), Support Vector Machine (SVM), Multivariate Adaptive Regression Splines (MARS), and Linear Discriminant Analysis (LDA), the data set, see Figure 2, was split into a training set that contained 211 samples (70% of the data) and a test set containing 90 samples (30% of the data) to be used for assessing the performance of the machine learning models used in this study. Because samples were selected at random for each class, the proportion of ornithopods and theropods is similar in training and test data set.

For each model, the hyperparameters were optimized to obtain the best possible results. For Logistic Regression (LR), a forward stepwise method was implemented, using the function step implemented in R (Hastie & Pregibon, 1992). In Forward Stepwise Regression, landmarks are iteratively added as the performance is assessed via the Akaike Information Criterion (AIC) (Akaike, 1974). The subset of 8 of the 20 landmarks selected in this way were 2, 4, 5, 9, 10, 15, 17, 20, see Figure 1.

For the MLP, the caret package was used to carry out a grid search of an MLP implemented in the nnet package. The number of neurons in the hidden layer were varied between 1 and 19 and the weight decay parameter λ was changed between 0 and 0.1. Both were optimized using Cohen's κ as the performance metric (Cohen, 1960), using a bootstrap resampling approach (Efron & Tibshirani, 1997). The resulting model had 17 hidden neurons and a weight decay parameter of $\lambda = 0.1$. For the Random Forest model, the number of randomly selected predictors was optimized using the caret package – the value reached was 4. The optimal SVM with a radial basis function kernel had parameters $\sigma = 0.010$, $C = 32$. LDA and MARS have no tuneable hyperparameters but prior probabilities for classifying a sample as an ornithopod or a theropod,

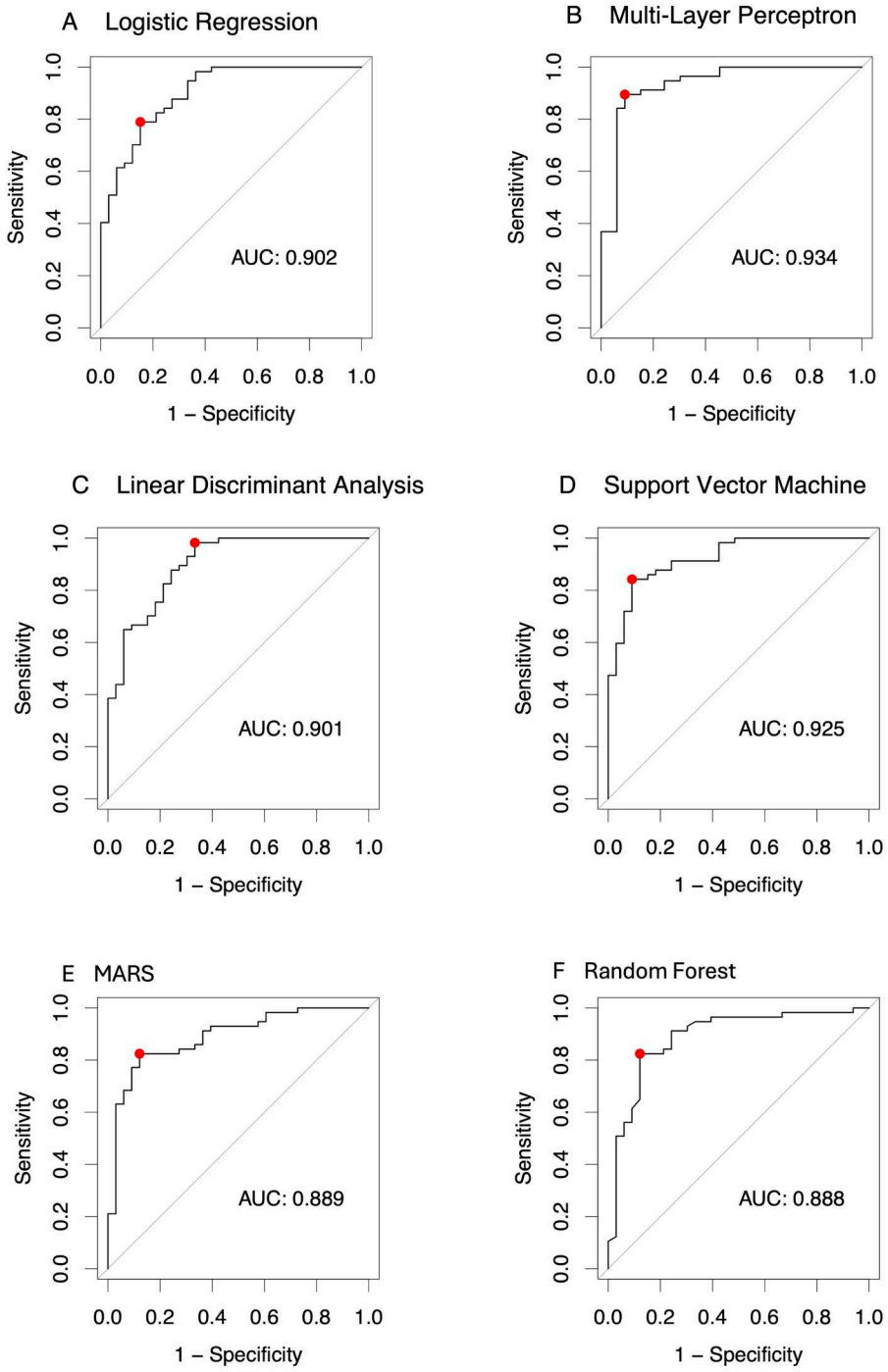

FIGURE 3. ROC curves for the machine learning methods used in this study. For each method, the Area under the Curve (AUC) has been calculated. The points on the ROC curve show the recall of theropods (sensitivity) and ornithopods (specificity) achieved by the optimal threshold.

respectively, have been set according to the proportions of each class.

After a model is fitted to the training set, its ability to correctly classify theropod and ornithopod footprints is assessed by the relative frequencies of correctly identified theropods (sensitivity) and ornithopods (specificity), respectively. Receiver Operating Characteristic (ROC) curves were generated for each model, see Figure 3. The ROC curve illustrates the trade-off of sensitivity and specificity. Increasing the performance of a classification method to identify theropods usually comes at the expense of its ability to recognize ornithopods and vice versa. By changing the threshold that determines which samples are classified as theropods versus ornithopods, sensitivity and specificity of a classification method can be varied. In Figure 3 we have indicated for each panel by a point on the ROC curve the sensitivity and specificity that can be achieved for a given method by optimizing the threshold. A summary statistic for ROC curves is the area under the ROC curve (AUROC) which provides a metric of the overall performance of a classifier.

Table 1 shows confusion matrices and performance metrics, Figure 4 shows the recall and accuracy for all methods both before and after optimizing the threshold using the ROC curves. All models show good accuracy scores between 80% and 90%. However, all methods except MLP are notably worse at

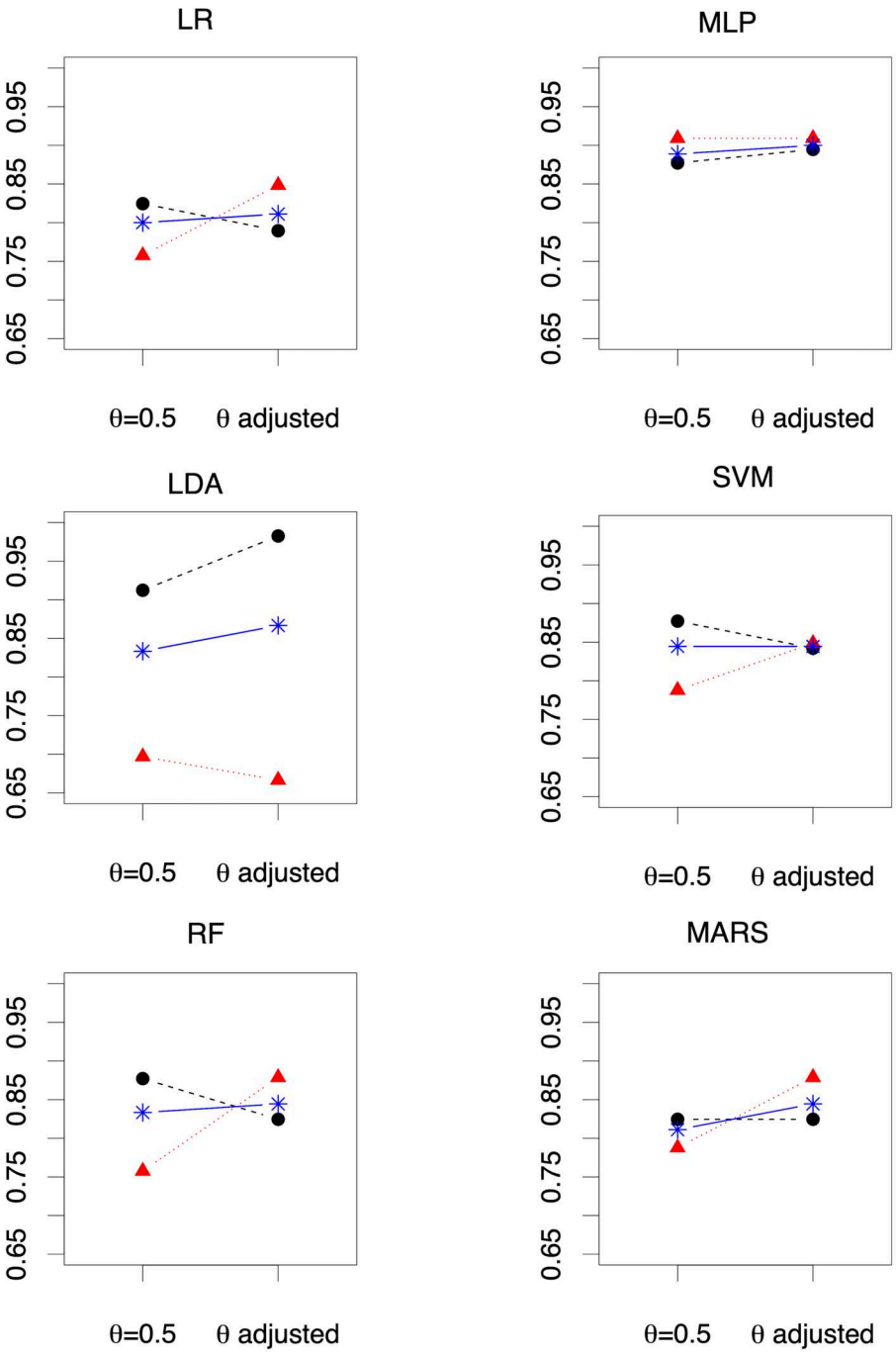

FIGURE 4. The plots show recall of ornithopods (triangles, dotted lines) and theropods (circles, dashed lines) as well as accuracy (asterisks, solid lines) for all methods before and after adjusting the threshold of the classifier. Recall quantifies the proportion of correctly classified samples of each type of dinosaur whereas accuracy is the overall percentage of correctly classified footprints.

accurately predicting the smaller class (i.e., ornithopods) before the threshold of the classifier is adjusted. After moving the threshold, most methods increase the recall of ornithopods whilst decreasing the recall of theropods. This is expected because there is a trade-off between both metrics, which is represented by the ROC curve. An exception to this pattern is LDA. Before adjusting the threshold, LDA has the best recall for theropods of any of the 6 methods (91.2%) whilst at the same time having the worst recall for ornithopods (69.7%). After adjusting the threshold, the recall of theropods increases whereas the recall of ornithopods decreases even further. As a result, LDA becomes an extreme case of a classifier that reaches a recall of 98.2% for theropods but at the expense of a very weak performance of classifying ornithopods, achieving a recall of only 66.7%. In contrast, even before adjusting the threshold, MLP's recall of ornithopods is already 90.9%, which remains unchanged after moving the threshold whilst the recall of theropods increases from 87.7% to 89.5%. Thus, MLP is not only the method that achieves the highest accuracy (90%) but also the highest recall for both classes. Because for this study performance should ideally be as high as possible for classifying both ornithopods and theropods, the MLP is superior to the other models.

Because we already achieved good performance after adjusting the thresholds of our models we did not attempt to address

the class imbalance further using data augmentation techniques such as undersampling, oversampling, or SMOTE.

DISCUSSION

Six machine learning methods were applied to the problem of distinguishing theropods and ornithopods, two groups of dinosaurs, based on footprints. Each footprint is represented by 20 landmarks which are placed as explained by Lallensack et al. (2020). Of the six models, MLP emerges as clearly superior in comparison to the other methods, achieving a recall for both classes of about 90%. We regard the fact that our models achieve good performance on a relatively small data set of around 300 samples a strength of our approach, it indicates that the representation by landmarks extracts meaningful information about the shape of the footprint and allows us to use computationally much less expensive machine learning models than in the approach proposed by some of the co-authors of this study in Lallensack et al. (2022) which, however, relied on silhouettes, black and white representations of footprint images. In the following we will discuss possible reasons for the benefits of reducing footprints to landmarks.

The system of 20 landmarks proposed by Lallensack et al. (2020) is based on a set of points of interest located on the boundaries of the footprints, such as the tips of the three toes (landmarks 1, 2, and 3) or the rear (landmark 4) of each footprint. One immediate advantage of using landmarks rather than working directly with image data is robustness to sources of error such as, for example, footprints that are located off-center or are rotated whilst, when determining the landmarks from images, distortions such as different orientations of a footprint with respect to the image frame are removed. As a result, using landmarks for building classifiers for distinguishing between theropods and ornithopods does not need to address the usual challenges faced in image processing applications. However, this suggests that the accuracy that can be achieved using machine learning models depend on how well the landmarks reflect the shape of each footprint.

Instead of using the two-dimensional coordinates (x, y) that indicate the locations of each landmark, we instead work with the distances $r = \sqrt{x^2 + y^2}$ of the landmarks from the center of the footprint. Thus, we reduce the number of variables from $2 \times 20 = 40$ coordinates to 20 distances from the center. From Figure 2 it seems intuitively clear that not much information is lost due to this transformation of the data set. This can be explained more rigorously by considering that rather than by two-dimensional cartesian coordinates (x, y), the locations of landmarks can equivalently be represented by polar coordinates (r, ϕ) i.e., by the distance r from the origin and an angle ϕ that indicates the direction where a point is located. Thus, our transformed data set can be described as a transformation to polar coordinates where the angular variable ϕ is omitted. Each landmark lies in a particular direction from the center. Landmark 2, the tip of the middle toe, lies above the center, whereas landmark 4 is located below. Landmark 1 is lateral (on the upper right), and landmark 2 is medial (on the upper left). Thus, because for different footprints each landmark is expected to be located in a similar direction from the center most of the information is contained in the distance r from the center and the angle ϕ can be omitted.

In fact, replacing the cartesian coordinates (x, y) by distances r from the center is essential for obtaining a set of variables that is suitable for training machine learning methods. When attempting to train various machine learning methods on the original data set, the fact is that some coordinates are not informative. For example, the x coordinate of landmark 2 is close to zero whereas the y coordinates of landmarks 5, 8, 10, 13, 17, and 20 are small, which causes problems and it is difficult to achieve convergence.

The number of variables can be reduced even further by variable selection. This was implemented for Logistic Regression via Forward Step Regression. The landmarks selected by forward regression shown by the solid circles in Figure 1 were among those that would intuitively be expected to be in the subset of the most informative landmarks: landmarks 2 and 4 as the tip and rear of the footprint, which are related to the length of a footprint, 5 and 10 that are linked to the width of the footprint, 17 and 20 that are halfway along the middle toe, and 9 at the beginning of the lateral (right) toe. Only landmark 15 seems slightly inconsistent with this pattern because it is the landmark next to landmark 2. Intuitively one might rather expect to find 14, the landmark opposite of 9, in the set of selected variables instead.

When fitting the other machine learning methods to the subset of variables selected by forward regression, the models obtained showed similar performance as when fitted to the full data set. Arguably that suggests that more parsimonious models could be obtained when reducing the modeling to the landmarks selected by forward selection. These results are presented in Supplementary Material, see Section "Results using variables selected by forward LR" of the Rmd and the PDF file.

We have also evaluated the performance metrics of all six machine learning methods on the training set, see Table 2. The metrics decrease on the test set (compare Table 1 and Table 2) as expected for a relatively small data set but remain high on the test set.

Finally, it is interesting to investigate the footprints that were misclassified in order to explore possible limitations of the approach, see Table 3. The references of the misclassified samples are: Barco et al., 2021; Castanera et al., 2013; Dalman & Weems, 2013; Ellenberger, 1974; Gierliński et al., 2004; Gierliński et al., 2009; Kim et al., 2018; Lallensack et al., 2016; Li et al., 2012; M. Lockley et al., 2008; Lockley & Meyer, 1998; Lockley et al., 1998; Lockley, 2010; M. G. Lockley et al., 2008; Lockley, Gierliński et al., 2014; Lockley, Honda et al., 2014; Matsukawa et al., 2006; Olsen, 1980; Olsen & Rainforth, 2003; Pittman, 1989; Raath, 1972; L. Xing et al., 2016; Xing et al., 2011; L. D. Xing et al., 2016; Xing, Lockley, Wand et al., 2014; Xing, Lockley, Zhang et al., 2014. Only two ornithopod and one theropod footprint were misclassified by all six machine learning models, see Figure 5A. The shapes of these three footprints, published by Castanera et al. (2013), Li et al. (2012), and Xing, Lockley, Zhang et al. (2014), reveal why it might be challenging to classify them correctly. For example, in all three figures the middle toe clearly points to the left or to the right, respectively, rather than straight ahead. Indeed, Castanera et al. (2013) argued that the tracks they described are challenging to refer to either group, and in this case the assignment to ornithopods could be made only because of the presence of manus tracks, though other works have attributed manus tracks to theropod trackmakers, e.g., Li et al. (2019) and Milner et al. (2009). The Li et al. (2012) track is referred to the ichnogenus *Anomoepus*, which is produced by small, basally branching ornithischians. In the absence of manus tracks, such tracks are generally difficult to assign to either theropods or ornithischians, and it is possible that the Li et al. (2012) track is a mis-identified theropod track.

The five footprints that have been misclassified by five out of six methods have been published in Castanera et al. (2013), Kim et al. (2018), Lockley (2010), Olsen and Rainforth (2003), and Xing et al. (2011). Looking at other misclassified footprints, for example, those shown in Figure 5C, it appears that the theropod footprints that have been misclassified by four out of six machine learning methods show characteristics that are more common for ornithopods. For Dalman and Weems (2013), Gierliński et al. (2009), Lallensack et al. (2016), Raath (1972), and Xing et al. (2014), the middle toe is relatively short and wide

TABLE 2. Six classification methods were trained on a training set of 211 samples of the data by Lallensack et al. (2020). Confusion matrices and recall (the percentage of correctly classified samples) were calculated for the same training set. Compare with the performance on the test set shown in Table 1.

Forward Stepwise Logistic Regression (LR)			Multi-Layer Perceptron (MLP)		
	Ornithopods	Theropods		Ornithopods	Theropods
Ornithopods	62	10	Ornithopods	71	2
Theropods	13	126	Theropods	4	134
Recall	82.7%	92.6%	Recall	94.7%	98.5%
Linear Discriminant Analysis (LDA)			**Random Forest (RF)**		
	Ornithopods	Theropods		Ornithopods	Theropods
Ornithopods	52	4	Ornithopods	75	0
Theropods	23	132	Theropods	0	136
Recall	69.3%	97.1%	Recall	100%	100%
Support Vector Machine (SVM)			**MARS**		
	Ornithopods	Theropods		Ornithopods	Theropods
Ornithopods	66	5	Ornithopods	63	7
Theropods	9	131	Theropods	12	129
Recall	88.0%	96.3%	Recall	84.0%	94.9%

TABLE 3. Samples in the data set that have been misclassified by one or more of the methods after adjusting the threshold. **Abbreviations**: **LDA**, linear discriminant analysis; **LR**, forward stepwise logistic regression; **MARS**, multivariate adaptive regression splines; **MLP**, multi-layer perceptron; **RF**, random forest; **SVM**, support vector machine.

Source	Ichnogenus	Epoch	Group	LDA	LR	MLP	RF	SVM	MARS	n
Barco et al. (2021)	*Iberosauripus*	Cretaceous	Early	✓	✓	✓	✓	✓	✗	1
Castanera et al. (2013)	NA	NA	NA	✗	✗	✗	✗	✗	✗	6
Castanera et al. (2013)	NA	NA	NA	✗	✗	✓	✗	✗	✗	5
Dalman and Weems (2013)	*Anomoepus*	Jurassic	Early	✗	✓	✗	✗	✓	✗	4
Ellenberger (1974)	*Moyenisauropus*	Jurassic	Early	✓	✓	✓	✓	✓	✗	1
Ellenberger (1974)	*Moyenisauropus*	Jurassic	Early	✗	✗	✓	✓	✗	✓	3
Ellenberger (1974)	*Moyenisauropus*	Jurassic	Early	✗	✗	✓	✓	✗	✓	3
Gierliński et al. (2004)	*Anomoepus*	Jurassic	Early	✗	✗	✓	✓	✗	✓	3
Gierliński et al. (2009)	*Therangospodus*	Jurassic	Middle	✓	✗	✓	✓	✗	✓	2
Gierliński et al. (2009)	*Carmelopodus*	Jurassic	Middle	✓	✓	✗	✗	✗	✗	4
Li et al. (2012)	*Anomoepus*	Jurassic	NA	✗	✗	✗	✗	✗	✗	6
Kim et al. (2018)	*Corpulentapus*	Cretaceous	Early	✓	✗	✗	✗	✗	✗	5
Lallensack et al. (2016)	NA	Cretaceous	Early	✓	✗	✗	✓	✗	✗	4
Lockley et al. (1998)	*Megalosauripus*	Jurassic	Late	✓	✓	✓	✗	✓	✗	2
Lockley et al. (1998)	*Therangospodus*	Jurassic	Late	✓	✓	✗	✓	✓	✓	1
M. G. Lockley et al. (2008)	*Hispanosauropus*	Jurassic	Late	✓	✓	✓	✗	✓	✓	1
M. Lockley et al. (2008)	*Minisauripus*	Cretaceous	Late	✗	✗	✓	✓	✗	✓	3
M. Lockley et al. (2008)	*Minisauripus*	Cretaceous	Early	✓	✗	✓	✓	✗	✓	2
Lockley (2010)	*Dinehichnus*	Jurassic	Early	✗	✗	✓	✗	✗	✗	5
Lockley (2010)	*Dinehichnus*	Jurassic	Early	✗	✓	✓	✓	✗	✓	2
Lockley, Gierliński, et al. (2014)	*Irenesauripus*	Cretaceous	NA	✓	✓	✓	✗	✓	✓	1
Lockley, Honda, et al. (2014)	NA	Cretaceous	NA	✓	✓	✓	✗	✓	✓	1
Matsukawa et al. (2006)	NA	Cretaceous	Early	✗	✓	✓	✓	✓	✓	1
Olsen (1980)	*Grallator*	Jurassic	Early	✓	✗	✓	✓	✗	✓	2
Olsen and Rainforth (2003)	*Anomoepus*	Jurassic	Early	✗	✗	✓	✗	✗	✗	5
Pittman (1989)	NA	Cretaceous	Early	✓	✓	✓	✓	✓	✗	1
Raath (1972)	NA	NA	NA	✗	✗	✓	✓	✗	✗	4
Xing et al. (2011)	*Kayentapus*	Cretaceous	Early	✗	✗	✗	✓	✗	✗	5
Xing, Lockley, Zhang, et al. (2014)	*Paracorpulentapus*	Cretaceous	Late	✗	✗	✗	✗	✗	✗	6
Xing, Lockley, Wand, et al. (2014)	NA	Jurassic	Early	✓	✓	✗	✗	✗	✗	4
L. D. Xing et al. (2016)	*Anomoepus*	Jurassic	Early	✓	✓	✓	✗	✓	✓	1
L. Xing et al. (2016)	*Minisauripus*	Cretaceous	Early	✓	✗	✓	✓	✗	✓	2

rather than long and thin. Again, some theropod tracks are very ornithopod-like in appearance, see Milner et al. (2023) for a particularly deceiving example.

These observations illustrate that, in contrast to a paleontologist who classifies a footprint, our approach relies only on the shape of a footprint, represented in a highly simplified format via 20 landmarks. Thus, our method should not be seen as an attempt to represent expert knowledge as faithfully as possible but rather as an effort to extract from the 20 landmarks the essential features of the geometry of an ornithopod footprint in contrast to a theropod footprint. The aim of our study was to answer the question if and how well ornithopod footprints can be distinguished from theropod footprints based on morphological features alone. We have demonstrated that despite deliberately restricting classification to geometric features whilst not accounting for criteria such as evidence for four-legged locomotion which would provide unequivocal evidence for an ornithopod footprint, we

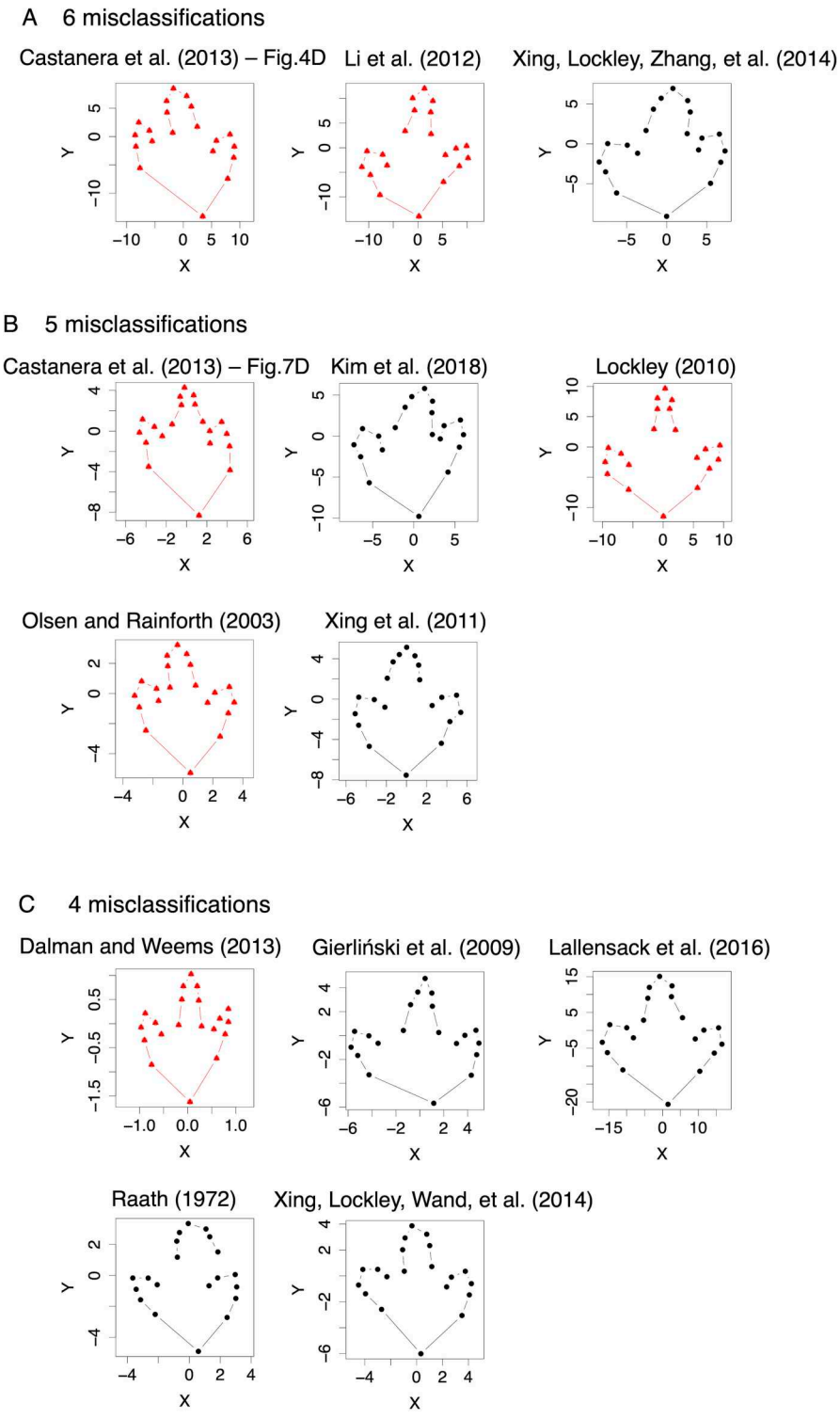

FIGURE 5. Footprints that are misclassified by all 6, 5, or 4 of the methods applied in this study. Ornithopod footprints are shown as triangles, theropods as filled circles. Note that the footprints shown here have different sizes. They are plotted on different scales to emphasize their shapes rather than their sizes.

achieve high recall for both ornithopod and theropod footprints which demonstrates that indeed, essential differences of the classes can be determined from the shape of the footprints alone.

It remains an interesting question, which could be studied in future work, how the machine learning approach proposed here relates to the classification carried out by paleontologists who rely on more comprehensive information than contained in the footprints alone. In some cases, for example, in the presence of manus footprints indicating a quadrupedal dinosaur these additional data, not accounted for by our machine learning approach, even determine unambiguously which class a dinosaur

belongs to. One possibility would be to identify samples for which irrefutable evidence exists to which class a footprint belongs to, either based on additional evidence or clear geometric features, and train the machine learning methods only on this part of the data. By determining the performance on footprints that are more ambiguous it could be tested to which extent the geometric features extracted by the machine learning methods are obtained from samples which have been classified with high certainty. However, investigating this important question would only be feasible by considerably augmenting the relatively small data set of our study. Because this requires annotating a substantial number of additional footprints with landmarks this question will be investigated in a future study.

CONCLUSION

We developed a machine learning approach for classifying ornithopod and theropod footprints using a data set consisting of 20 landmarks that describe the shape of the footprints. We achieve accuracies of above 80% up to 90% for MLP, the best-performing method. MLP also shows a balanced performance for both classes, achieving recalls of approximately 90% for both ornithopods and theropods.

ACKNOWLEDGMENTS

JNL was supported by the Alexander von Humboldt-Foundation, Bonn, Germany. PLF was supported by a UKRI Frontier Research Grant TRACKEVOL (selected by the ERC as a consolidator award).

AUTHOR CONTRIBUTIONS

IS, JNL, PLF, and IJ designed the project. MJ and IS carried out the project and wrote the first draft of the manuscript. All authors reviewed and approved the manuscript.

DATA AVAILABILTY STATEMENT

All data and the code necessary for replicating the findings of this study can be found in the Supplementary Material. The full data set is found in the file DinoPrints.csv, all code used for this study is included in the R Markdown file: SupplementaryMaterial_JournalVertebratePalaeontology2025.Rmd.

DISCLOSURE STATEMENT

No potential conflict of interest was reported by the author(s).

ORCID

Jens N. Lallensack http://orcid.org/0000-0003-4104-5232
Ian Jarman http://orcid.org/0000-0003-1932-4948
Peter L. Falkingham http://orcid.org/0000-0003-1856-8377
Ivo Siekmann http://orcid.org/0000-0002-0706-6307

SUPPLEMENTARY FILE(S)

SupplementaryMaterial_Journal

VertebratePalaeontology2025.Rmd: R Markdown implementation of the machine learning methods used for this study.

SupplementaryMaterial_JournalVertebrate

Palaeontology2025.PDF: Report generated from R Markdown file.

DinoPrints.csv: Data set of ornithopod and theropod footprints (Lallensack et al., 2020).

LITERATURE CITED

Akaike, H. (1974). A new look at the statistical model identification. *IEEE Transactions on Automatic Control*, *19*(6), 716–723. https://doi.org/10.1109/TAC.1974.1100705

Barco, J. L., Canudo, J. I., Ruiz-Omeñaca, J. I., & Rubio, J. L. (2021). Evidencia icnológica de un dinosaurio terópodo gigante en el Berriasiense (Cretácico Inferior) de Laurasia (las Villasecas, Soria, España). *Spanish Journal of Palaeontology*, *20*(3), 59–71. https://doi.org/10.7203/sjp.20.3.20580

Castanera, D., Pascual, C., Razzolini, N. L., Vila, B., Barco, J. L., & Canudo, J. I. (2013). Discriminating between Medium-Sized Tridactyl Trackmakers: Tracking Ornithopod Tracks in the Base of the Cretaceous (Berriasian, Spain). *PLoS ONE*, *8*(11), e81830. https://doi.org/10.1371/journal.pone.0081830

Cohen, J. (1960). A Coefficient of Agreement for Nominal Scales. *Educational and Psychological Measurement*, *20*(1), 37–46. https://doi.org/10.1177/001316446002000104

Dalman, S. G., & Weems, R. E. (2013). A new look at morphological variation in the ichnogenus *Anomoepus*, with special reference to material from the Lower Jurassic Newark Supergroup: implications for ichnotaxonomy and ichnodiversity. *Bulletin of the Peabody Museum of Natural History*, *54*(1), 67–124. https://doi.org/10.3374/014.054.0104

Demathieu, G. R. (1990). Problems in discrimination of tridactyl dinosaur footprints, exemplified by the Hettangian trackways, the causses, France. *Ichnos*, *1*(2), 97–110. https://doi.org/10.1080/10420949009386339

dePolo, P. E., Brusatte, S. L., Challands, T. J., Foffa, D., Wilkinson, M., Clark, N. D. L., Hoad, J., Pereira, P. V. L. G. d. C., Ross, D. A., & Wade, T. J. (2020). Novel track morphotypes from new tracksites indicate increased Middle Jurassic dinosaur diversity on the Isle of Skye, Scotland. *PLoS ONE*, *15*(3), e0229640. https://doi.org/10.1371/journal.pone.0229640

Efron, B., & Tibshirani, R. (1997). Improvements on Cross-Validation: The 632+ Bootstrap Method. *Journal of the American Statistical Association*, *92*(438), 548–560. https://doi.org/10.1080/01621459.1997.10474007

Ellenberger, P. (1974). Contribution a la classification des pistes de vertébrés du Trias: les types du Stormberg d'Afrique du Sud (II ème partie: Le Stormberg Superieur– I. Le biome de la zona B/1 ou niveau de Moyeni: ses biocénoses). *Palaeovertebrata, Memoire Extraordinaire*, 1–143.

Falkingham, P. (2014). Interpreting ecology and behaviour from the vertebrate fossil track record. *Journal of Zoology*, *292*(4), 222–228. doi:10.1111/jzo.12110

Falkingham, P., Marty, D., & Richter, A. (2016). Applying objective methods to subjective track outlines. In *Dinosaur tracks: the next steps* (pp. 72–81). Indiana University Press.

Falkingham, P. L., Bates, K. T., Avanzini, M., Bennett, M., Bordy, E. M., Breithaupt, B. H., Castanera, D., Citton, P., Díaz-Martínez, I., Farlow, J. O., Fiorillo, A. R., Gatesy, S. M., Getty, P., Hatala, K. G., Hornung, J. J., Hyatt, J. A., Klein, H., Lallensack, J. N., Martin, A. J., Marty, D., Matthews, N. A., Meyer, C. A., Milàn, J., Minter, N. J., Razzolini, N. L., Romilio, A., Salisbury, S. W., Sciscio, L., Tanaka, I., Wiseman, A. L. A., Xing, L. D., & Belvedere, M. (2018). A standard protocol for documenting modern and fossil ichnological data. *Palaeontology*, *61*(4), 469–480. https://doi.org/https://doi.org/10.1111pala.12373

Figueiredo, S., Dinis, P., Belo, J., Rosina, P., & Strantzali, I. B. (2017). A new record of a possible ornithopod footprint from the Lower Cretaceous of Cabo Espichel (Sesimbra, Portugal). *Bollettino della Società Paleontologica Italiana*, *56*(2), 217–231. https://doi.org/10.4435/BSPI.2017.20

Gierliński, G., Pieńkowski, G., & Niedźwiedzki, G. (2004). Tetrapod Track Assemblage in the Hettangian of Sołtyków, Poland, and its Paleoenvironmental Background. *Ichnos*, *11*(3-4), 195–213. https://doi.org/10.1080/10420940490444861

Gierliński, G. G., Menducki, P., Janiszewska, K., Wicik, I., & Boczarowski, A. (2009). A preliminary report on dinosaur track assemblages from the Middle Jurassic of the Imilchil area, Morocco [Dinosaur tracks; Bathonian; Bajocian; Central High Atlas; Morocco]. *Geological Quarterly*, *53*(4), 6. https://gq.pgi.gov.pl/article/view/7964

Härdle, W. K., & Simar, L. (2014). *Applied Multivariate Statistical Analysis (4 ed.)*. Springer.

Hastie, T., Tibshirani, R., Friedman, J. H., & Friedman, J. H. (2009). *The elements of statistical learning: data mining, inference, and prediction (Vol. 2)*. Springer.

Hastie, T. J., & Pregibon, D. (1992). Generalized linear models. In J. M. Chambers, & T. J. Hastie (Eds.), *Statistical Models in S*. Wadsworth & Brooks/Cole.

Kim, K. S., Lim, J. D., Lockley, M. G., Xing, L., Ha, S. J., Kim, C. B., Paik, I. S., Ahn, J. H., & Mun, S. C. (2018). First reports of a distinctive theropod track assemblage from the Jinju Formation (Lower Cretaceous) of Korea provides strong correlations with China. *Cretaceous Research*, *81*, 26–35. https://doi.org/https://doi.org/10.1016j.cretres.2017.08.005

Lallensack, J. N. (2019). Automatic generation of objective footprint outlines. *PeerJ*, *7*, e7203. doi:10.7717/peerj.7203

Lallensack, J. N., Engler, T., & Barthel, H. J. (2020). Shape variability in tridactyl dinosaur footprints: the significance of size and function. *Palaeontology*, *63*(2), 203–228. doi:10.1111/pala.12449

Lallensack, J. N., Leonardi, G., & Falkingham, P. L. (2025). Glossary of fossil tetrapod tracks. *Palaeontologia Electronica*, *27*, 1-105. https://doi.org/10.26879/1389

Lallensack, J. N., Romilio, A., & Falkingham, P. L. (2022). A machine learning approach for the discrimination of theropod and ornithischian dinosaur tracks. *Journal of the Royal Society Interface*, *19*(196), https://doi.org/10.1098/rsif.2022.0588

Lallensack, J. N., van Heteren, A. H., & Wings, O. (2016). Geometric morphometric analysis of intratrackway variability: a case study on theropod and ornithopod dinosaur trackways from Münchehagen (Lower Cretaceous, Germany). *PeerJ*, *4*, e2059. doi:10.7717/peerj.2059

Li, D.-Q., Xing, L.-D., Lockley, M. G., Romilio, A., Yang, J.-T., & Li, L.-F. (2019). The first theropod tracks from the Middle Jurassic of Gansu, Northwest China: new and rare evidence of quadrupedal progression in theropod dinosaurs. *Journal of Palaeogeography*, *8*(1), 10. https://doi.org/10.1186/s42501-019-0028-4

Li, J., Lockley, M. G., Zhang, Y., Hu, S., Matsukawa, M., & Bai, Z. (2012). An Important Ornithischian Tracksite in the Early Jurassic of the Shenmu Region, Shaanxi, China. *Acta Geologica Sinica - English Edition*, *86*(1), 1–10. https://doi.org/https://doi.org/10.1111j.1755-6724.2012.00606.x

Lockley, M., Kim, J., Kim, K. S., Kim, S., Matsukawa, M., Rihui, L., Jianjun, L., & Yang, S.-Y. (2008). *Minisauripus*—the track of a diminutive dinosaur from the Cretaceous of China and South Korea: implications for stratigraphic correlation and theropod foot morphodynamics. *Cretaceous Research*, *29*(1), 115–130. https://doi.org/10.1016/j.cretres.2007.04.003

Lockley, M., & Meyer, C. (1998). Therangospodus: Trackway evidence for the widespread distribution of a Late Jurassic theropod with well-padded feet. *GAIA*, *15*.

Lockley, M., Meyer, C., & Faria dos Santos, V. (1998). *Megalosauripus* and the problematic concept of Megalosaur footprints. *GAIA*, *15*, 313–337.

Lockley, M. G. (2010). New perspectives on morphological variation in tridactyl footprints: clues to widespread convergence in developmental dynamics. *Geological Quarterly; Vol 53, No 4 (2009)*. https://gq.pgi.gov.pl/article/view/7530.

Lockley, M. G., Garcia-Ramos, J. C., Piñuela, L., & Avanzini, M. (2008). A review of vertebrate track assemblages from the Late Jurassic of Asturias, Spain with comparative notes on coeval ichnofaunas from the western USA: implications for faunal diversity in siliciclastic facies assemblages. *Oryctos*, *8*, 53–70.

Lockley, M. G., Gierliński, G. D., Martin, J., & Kent, C. (2014). An unusual theropod tracksite in the Cretaceous Dakota Group, western Colorado: Implications for ichnodiversity. In M. G. Lockley, & S. G. Lucas (Eds.), *Fossil footprints of western North America* (pp. 411–415.

Lockley, M. G., Honda, K. K., & Simmons, B. (2014). A new dinosaur tracksite in the Dakota Group (Cretaceous) of the historic Stone City area, Colorado. In M. G. Lockley, & S. G. Lucas (Eds.), *Fossil footprints of western North America* (pp. 205–210.

Mateus, O. v., & Milàn, J. (2008). Ichnological evidence for giant ornithopod dinosaurs in the Upper Jurassic Lourinhã Formation, Portugal. *Oryctos*, *8*, 47–52.

Matsukawa, M., Lockley, M., & Jianjun, L. (2006). Cretaceous terrestrial biotas of East Asia, with special reference to dinosaur-dominated ichnofaunas: towards a synthesis. *Cretaceous Research*, *27*(1), 3–21. https://doi.org/https://doi.org/10.1016j.cretres.2005.10.009

Milner, A., Santucci, V., Wood, J., Birthisel, T., Clites, E., & Lockley, M. (2023). The John Wesley Powell Fossil Track Block—theropod tracks with ornithopod-like morphology from the Early Jurassic Navajo Sandstone, Glen Canyon National Recreation Area, Utah-Arizona. *Geology of the Intermountain West*, *10*, 185–222. https://doi.org/10.31711/giw.v10.pp185-222

Milner, A. R. C., Harris, J. D., Lockley, M. G., Kirkland, J. I., & Matthews, N. A. (2009). Bird-Like Anatomy, Posture, and Behavior Revealed by an Early Jurassic Theropod Dinosaur Resting Trace. *PLOS ONE*, *4*(3), e4591. https://doi.org/10.1371/journal.pone.0004591

Moratalla, J. J., Sanz, J. L., & Jimenez, S. (1988). Multivariate analysis on Lower Cretaceous dinosaur footprints: discrimination between ornithopods and theropods. *Geobios*, *21*(4), 395–408. doi:10.1016/S0016-6995(88)80042-1

Olsen, P. (1980). Fossil great lakes of the Newark Supergroup in New Jersey. *Field Studies of New Jersey Geology and Guide to Field Trips*.

Olsen, P., & Rainforth, E. (2003). The Early Jurassic ornithischian dinosaurian ichnogenus *Anomoepus*. In P. M. LeTourneau, & P. E. Olsen (Eds.), *The Great Rift Valleys of Pangea in Eastern North America (Vol. 2* (pp. 314–367). Columbia University Press.

Piñuela, L., García-Ramos, J. C., Romano, M., & Ruiz-Omeñaca, J. I. (2016). First Record of Gregarious Behavior in Robust Medium-Sized Jurassic Ornithopods: Evidence from the Kimmeridgian Trackways of Asturias (N. Spain) and Some General Considerations on Other Medium-Large Ornithopod Tracks in the Mesozoic Record. *Ichnos*, *23*(3-4), 298–311. https://doi.org/10.1080/10420940.2016.1178640

Pittman, J. G. (1989). Stratigraphy, lithology, depositional environment, and track type of dinosaur track-bearing beds of the Gulf Coastal Plain. *Dinosaur tracks and traces*. https://bib.rero.ch/global/documents/764756.

R Core Team. (2023). *R: a language and environment for statistical computing*. R Foundation for Statistical Computing, Vienna, Austria. Retrieved 20th October 2023 from https://www.R-project.org

Raath, M. A. (1972). First record of dinosaur footprints from Rhodesia. *Arnoldia (Rhodesia) Series of Miscellaneous Publications National Museums of Rhodesia*, *5*, 1–5.

Romilio, A., & Salisbury, S. W. (2011). A reassessment of large theropod dinosaur tracks from the mid-Cretaceous (late Albian–Cenomanian) Winton Formation of Lark Quarry, central-western Queensland, Australia: A case for mistaken identity. *Cretaceous Research*, *32*(2), 135–142. https://doi.org/https://doi.org/10.1016j.cretres.2010.11.003

Romilio, A., & Salisbury, S. W. (2014). Large dinosaurian tracks from the Upper Cretaceous (Cenomanian-Turonian) portion of the Winton Formation, Lark Quarry, central-western Queensland, Australia: 3D photogrammetric analysis renders the 'stampede trigger' scenario unlikely. *Cretaceous Research*, *51*, 186–207. https://doi.org/10.1016/j.cretres.2014.06.003

Romilio, A., Tucker, R. T., & Salisbury, S. W. (2013). Reevaluation of the Lark Quarry Dinosaur Tracksite (Late Albian-Cenomanian Winton Formation, Central-Western Queensland, Australia): No longer a stampede? *Journal of Vertebrate Paleontology*, *33*(1), 102–120. doi:10.1080/02724634.2012.694591

Schulp, A. S., & Al-Wosabi, M. (2012). Telling apart ornithopod and theropod trackways: A closer look at a large, Late Jurassic tridactyl dinosaur trackway at Serwah, Republic of Yemen. *Ichnos*, *19*(4), 194–198. https://doi.org/10.1080/10420940.2012.710672

Thulborn, R. A. (2013). Lark Quarry revisited: a critique of methods used to identify a large dinosaurian track-maker in the Winton Formation (Albian–Cenomanian), western Queensland, Australia. *Alcheringa: An Australasian Journal of Palaeontology*, *37*(3), 312–330. https://doi.org/10.1080/03115518.2013.748482

Thulborn, R. A., & Wade, M. (1979). Dinosaur Stampede in the Cretaceous of Queensland. *Lethaia*, *12*(3), 275–279. doi:10.1111/j.1502-3931.1979.tb01008.x

Thulborn, T., & Wade, M. (1984). Dinosaur trackways in the Winton Formation (mid-Cretaceous) of Queensland. *Memoirs of the Queensland Museum*, *21*, 413–517.

Xing, L., Lockley, M. G., Yang, G., Cao, J., Benton, M., Xu, X., Zhang, J., Klein, H., Persons, W. S., Kim, J. Y., Peng, G., Ye, Y., & Ran, H. (2016). A new Minisauripus site from the Lower Cretaceous of China: Tracks of small adults or juveniles? *Palaeogeography,*

Palaeoclimatology, Palaeoecology, *452*, 28–39. doi:10.1016/j.palaeo.2016.04.006

Xing, L. D., Harris, J. D., Jia, C.-K., Luo, Z.-J., Wang, S.-N., & An, J.-F. (2011). Early cretaceous bird-dominated and dinosaur footprint assemblages from the northwestern margin of the Junggar Basin, Xinjiang, China. *Palaeoworld*, *20*(4), 308–321. https://doi.org/https://doi.org/10.1016j.palwor.2011.01.001

Xing, L. D., Lockley, M. G., Hu, S., Li, Q., & Persons, W. S. (2016). Early Jurassic *Anomoepus* tracks from the Fengjiahe Formation of northern Central Yunnan, China. In R. M. Sullivan, & S. G. Lucas (Eds.), *Fossil Record 5 (Vol. 5* (pp. 327–330.

Xing, L. D., Lockley, M. G., Wand, Q.-F., Li, Z.-D., Klein, H., IV, W. S. P., Ye, Y., & Matsukawa, M. (2014). Earliest records of dinosaur footprints in Xinjiang, China. *Vertebrata PalAsiatica*, *52*, 340–348.

Xing, L. D., Lockley, M. G., Zhang, J. P., Klein, H., Kim, J. Y., Persons, W. S., Matsukawa, M., Yu, X. Q., Li, J. J., Chen, G. B., & Hui, Y. (2014). Upper Cretaceous dinosaur track assemblages and a new theropod ichnotaxon from Anhui Province, eastern China. *Cretaceous Research*, *49*, 190–204. https://doi.org/10.1016/j.cretres.2014.03.003

Handling Editor: Daniel Madzia.